



Gas gain stabilisation in the ATLAS TRT detector

Mindur, B.; Akesson, T. P. A.; Anghinolfi, F.; Antonov, Anton; Arslan, O.; Baker, O. K.; Banas, E.; Bault, C.; Beddall, A. J.; Bendotti, J.; Benjamin, D. P.; Bertelsen, H.; Bingul, A.; Bocci, A.; Boldyrev, A. S.; Brock, I.; Garrido, M. Capeans; Catinaccio, A.; Celebi, E.; Cetin, S. A.; Choi, John K.; Dam, Mogens; Danielsson, H.; Davis, D. R.; Degeorge, C.; Derendarz, D.; Desch, K.; Di Girolamo, B.; Dittus, F.; Dixon, Nicholas E.; Dressnandt, N.; Dubinin, F. A.; Evans, David H.; Farthouat, P.; Fedin, O. L.; Froidevaux, D.; Gavrilenko, I. L.; Gay, C.; Gecse, Z.; Godlewski, J.; Greife, C.; Gurbuz, S.; Hajduk, Z.; Hance, M.; Haney, B.; Hansen, Jørgen Beck; Hansen, P. H.; Hawkins, A. D.; Heim, S.; Holway, K.; Kantserov, V. A.; Katounine, S.; Kayumov, F.; Keener, P. T.; Kisielewski, B.; Klopov, N. V.; Konovalov, S. P.; Koperny, S.; Korotkova, N. A.; Kowalski, T. Z.; Kramarenko, V.; Krasnopevtsev, D.; Kruse, M.; Kudin, L. G.; Lichard, P.; Loginov, A.; Martinez, N. Lorenzo; Lucotte, A.; Luehring, F.; Lytken, E.; Maleev, V. P.; Maevskiy, A. S.; Ramos, J. Manjarres; Mashinistov, R. Y.; Meyer, C.; Mialkovski, V.; Mistry, K.; Mitsou, V. A.; Nadtochi, A. V.; Newcomer, F. M.; Novodvorski, E. G.; Ogren, H.; Oh, S. H.; Oleshko, S. B.; Olszowska, J.; Ostrowicz, W.; Palacino, G.; Patrichev, S.; Penwell, J.; Perez-Gomez, Francisco; Peshekhonov, V. D.; Rohne, O.; Reilly, M. B.; Ricken, O.; Rousseau, D.; Shmeleva, A. P.; Shulga, E.; Sivoklov, S.; Smirnov, S.; Smirnov, Yu.; Smirnova, L. N.; Soldatov, E.; Sulin, V. V.; Tartarelli, G.; Taylor, W.; Thomson, E.; Tikhomirov, V. O.; Tipton, P.; Valls Ferrer, J. A.; van den Berg, Ria; Vasquez, Juan Luis; Vasilyeva, L. F.; Vlazlo, O.; Weinert, B.; WILLIAMS, H.; Wong, [No Value]; Zhukov, K. I.; Zieminska, D.

Published in:
Journal of Instrumentation

DOI:
[10.1088/1748-0221/11/04/P04027](https://doi.org/10.1088/1748-0221/11/04/P04027)

Publication date:
2016

Document version
Publisher's PDF, also known as Version of record

Gas gain stabilisation in the ATLAS TRT detector

This content has been downloaded from IOPscience. Please scroll down to see the full text.

2016 JINST 11 P04027

(<http://iopscience.iop.org/1748-0221/11/04/P04027>)

View [the table of contents for this issue](#), or go to the [journal homepage](#) for more

Download details:

IP Address: 130.225.212.4

This content was downloaded on 27/04/2017 at 12:00

Please note that [terms and conditions apply](#).

You may also be interested in:

[The ATLAS TRT Barrel Detector](#)

The ATLAS TRT collaboration, E Abat, T N Addy et al.

[Combined performance tests before installation of the ATLAS Semiconductor and Transition Radiation Tracking Detectors](#)

E Abat, A Abdesselam, T N Addy et al.

[A double-sided silicon micro-strip Super-Module for the ATLAS Inner Detector upgrade in the High-Luminosity LHC](#)

S Gonzalez-Sevilla, A A Affolder, P P Allport et al.

[Measurement of the ATLAS solenoid magnetic field](#)

M Aleksa, F Bergsma, P -A Giudici et al.

[The ATLAS TRT and its Performance at LHC](#)

Ahmet Bingöl

[The ATLAS TRT end-cap detectors](#)

The ATLAS TRT collaboration, E Abat, T N Addy et al.

[The detector control system of the ATLAS SemiConductor Tracker during macro-assembly and integration](#)

A Abdesselam, A Barr, S Basiladze et al.

[Studies of the CMS electromagnetic calorimeter performance in the electron test beam](#)

Roberta Arcidiacono and the CMS ECAL Group

Gas gain stabilisation in the ATLAS TRT detector

The ATLAS TRT collaboration

B. Mindur,^{h,1} T.P.A. Åkesson,ⁿ F. Anghinolfi,^f A. Antonov,^q O. Arslan,^e O.K. Baker,^y E. Banas,ⁱ C. Bault,^f A.J. Beddall,^a J. Bendotti,^f D.P. Benjamin,^j H. Bertelsen,^g A. Bingul,^b A. Bocci,^j A.S. Boldyrev,^r I. Brock,^e M. Capeáns Garrido,^f A. Catinaccio,^f E. Celebi,^c S.A. Cetin,^d K. Choi,^l M. Dam,^g H. Danielsson,^f D. Davis,^j C. Degeorge,^l D. Derendarz,ⁱ K. Desch,^e B. Di Girolamo,^f F. Dittus,^f N. Dixon,^f N. Dressnandt,^u F.A. Dubinin,^p H. Evans,^l P. Farthouat,^f O.L. Fedin,^v D. Froidevaux,^f I.L. Gavrilenko,^p C. Gay,^x Z. Gecse,^x J. Godlewski,ⁱ C. Greife,^e S. Gurbuz,^c Z. Hajduk,ⁱ M. Hance,^u B. Haney,^u J.B. Hansen,^g P.H. Hansen,^g A.D. Hawkins,ⁿ S. Heim,^u K. Holway,^j V.A. Kantserov,^q S. Katounine,^v F. Kayumov,^p P.T. Keener,^u B. Kisielewski,ⁱ N.V. Klopov,^v S.P. Konovalov,^p S. Koperny,^h N.A. Korotkova,^r T.Z. Kowalski,^h V. Kramarenko,^r D. Krasnopevtsev,^q M. Kruse,^j L.G. Kudin,^v P. Lichard,^f A. Loginov,^y N. Lorenzo Martinez,^l A. Lucotte,^k F. Luehring,^l E. Lytken,ⁿ V.P. Maleev,^v A.S. Maevskiy,^r J. Manjarres Ramos,^z R.Y. Mashinistov,^p C. Meyer,^u V. Mialkovski,^m K. Mistry,^u V.A. Mitsou,^w A.V. Nadtochi,^v F.M. Newcomer,^u E.G. Novodvorski,^v H. Ogren,^l S.H. Oh,^j S.B. Olesko,^v J. Olszowska,ⁱ W. Ostrowicz,ⁱ G. Palacino,^z S. Patrichev,^v J. Penwell,^l F. Perez-Gomez,^f V.D. Peshekhonov,^m O. Røhne,^t M.B. Reilly,^u C. Rembser,^f O. Ricken,^e A. Romaniouk,^q D. Rousseau,^s V. Ryjov,^m U. Sasmaz,^b S. Schaepe,^e V.A. Schegelsky,^v A.P. Shmeleva,^p E. Shulga,^q S. Sivoklokov,^r S. Smirnov,^q Yu. Smirnov,^q L.N. Smirnova,^r E. Soldatov,^q V.V. Sulin,^p G. Tartarelli,^o W. Taylor,^z E. Thomson,^u V.O. Tikhomirov,^p P. Tipton,^y J.A. Valls Ferrer,^w R. Van Berg,^u J. Vasquez,^y L.F. Vasilyeva,^p O. Vlazlo,ⁿ B. Weinert,^l H.H. Williams,^u V. Wong,^x K.I. Zhukov^p and D. Zieminska^l

^aBahcesehir University, Faculty of Engineering and Natural Sciences, 34353, Besiktas, Istanbul, Turkey

^bGaziantep University, Department of Physics Engineering, 27300, Sehitkamil, Gaziantep, Turkey

^cBogazici University, Department of Physics, 34342, Bebek, Istanbul, Turkey

^dIstanbul Bilgi University, Faculty of Engineering and Natural Sciences, 34060, Eyup, Istanbul, Turkey

^ePhysikalisches Institut, University of Bonn, Bonn, Germany

^fCERN, CH - 1211 Geneva 23, Switzerland, Switzerland

^gNiels Bohr Institute, University of Copenhagen, Blegdamsvej 17, DK - 2100 Kobenhavn 0, Denmark

^hFaculty of Physics and Applied Computer Science of the AGH-University of Science and Technology, (FPACS, AGH-UST), al. Mickiewicza 30, PL-30059 Cracow, Poland

¹Corresponding author.



ⁱHenryk Niewodniczanski Institute of Nuclear Physics, Polish Academy of Sciences,
ul. Radzikowskiego 152, PL - 31342 Cracow, Poland

^jDuke University, Department of Physics, Durham, NC 27708, U.S.A.

^kLaboratoire de Physique Subatomique et de Cosmologie, CNRS-IN2P3, Université Joseph Fourier, INPG,
53 avenue des Martyrs, FR - 38026 Grenoble Cedex, France

^lIndiana University, Department of Physics,
Swain Hall West, Room 117, 727 East Third St., Bloomington, IN 47405-7105, U.S.A.

^mJoint Institute for Nuclear Research, JINR Dubna, RU - 141 980 Moscow Region, Russia

ⁿLunds Universitet, Fysiska Institutionen, Box 118, SE - 221 00 Lund, Sweden

^oINFN Milano and Università di Milano, Dipartimento di Fisica, via Celoria 16, IT - 20133 Milano, Italy

^pP.N. Lebedev Institute of Physics, Academy of Sciences, Leninsky pr. 53, RU - 117 924 Moscow, Russia

^qNational Research Nuclear University MEPhI, Kashirskoe Shosse 31, RU -115409 Moscow, Russia

^rLomonosov Moscow State University, Skobeltsyn Institute of Nuclear Physics,
RU - 119 992 Moscow Lenskie gory 1, Russia

^sLAL, Univ. Paris-Sud, IN2P3/CNRS, Orsay, France

^tDepartment of Physics, University of Oslo, Blindern, NO - 0316 Oslo 3, Norway

^uUniversity of Pennsylvania, Department of Physics & Astronomy,
209 S. 33rd Street, Philadelphia, PA 19104, U.S.A.

^vPetersburg Nuclear Physics Institute, RU - 188 300 Gatchina, Russia

^wInstituto de Física Corpuscular (IFIC), Centro Mixto UVEG-CSIC, Apdo. 22085, ES-46071 Valencia;
Dept. Física At., Mol. y Nuclear, Univ. of Valencia and Instituto de Microelectrónica de Barcelona
(IMB-CNM-CSIC), 08193 Bellaterra, Barcelona, Spain

^xUniversity of British Columbia, Department of Physics,
6224 Agriculture Road, CA - Vancouver, B.C. V6T 1Z1, Canada

^yYale University, Department of Physics, PO Box 208121, New Haven CT, 06520-8121, U.S.A.

^zYork University, Department of Physics and Astronomy, Toronto ON, Canada

E-mail: bartosz.mindur@agh.edu.pl

ABSTRACT: The ATLAS (one of two general purpose detectors at the LHC) Transition Radiation Tracker (TRT) is the outermost of the three tracking subsystems of the ATLAS Inner Detector. It is a large straw-based detector and contains about 350,000 electronics channels. The performance of the TRT as tracking and particularly particle identification detector strongly depends on stability of the operation parameters with most important parameter being the gas gain which must be kept constant across the detector volume. The gas gain in the straws can vary significantly with atmospheric pressure, temperature, and gas mixture composition changes. This paper presents a concept of the gas gain stabilisation in the TRT and describes in detail the Gas Gain Stabilisation System (GGSS) integrated into the Detector Control System (DCS). Operation stability of the GGSS during Run-1 is demonstrated.

KEYWORDS: Gaseous detectors; Particle tracking detectors (Gaseous detectors); Transition radiation detectors; Wire chambers (MWPC, Thin-gap chambers, drift chambers, drift tubes, proportional chambers etc)

Contents

1	Introduction	1
2	Gas gain stabilisation in the ATLAS TRT	3
3	Operation principles of the Gas Gain Stabilisation System	5
4	Properties of the reference straw tubes and related components	7
4.1	Gas gain measurements	7
4.2	Gas gain temperature dependence	9
5	Design of the Gas Gain Stabilisation System	9
5.1	Hardware	9
5.2	Software	11
6	Longterm system performance	12
6.1	Reference high voltage	12
6.2	Gas gain stability	13
7	Conclusions	14

1 Introduction

The ATLAS Inner Detector (ID) is composed of three detector sub-systems: the silicon-based Pixel and SemiConductor Tracker (SCT) detectors, and the gaseous drift tube (straw) based Transition Radiation Tracker (TRT) [1]. Schematically the design of the ATLAS Inner detector is shown in figures 1 and 2.

The TRT is the outermost of the three sub-systems (see [2–4] for more details). The active region of the TRT detector contains 298,304 straw drift tubes of 4 mm diameter (350,848 electronics channels). The barrel section of the TRT covers $560 < R < 1080$ mm and $|z| < 720$ mm and has the straws aligned parallel to the direction of the beam axis. The two end-cap sections cover $827 < |z| < 2744$ mm and $617 < R < 1106$ mm and have the straws arranged radially in wheels.

The TRT exploits a novel design which combines continuous tracking capability with particle identification (PID) based on transition radiation (TR). The latter functionality provides substantial discriminating power between electrons and pions over the energy range between 1 and 100 GeV and is a crucial component of the ‘tight’ electron selection criteria in ATLAS. The TRT straws are filled with a gas mixture of 70% Xe, 27% CO₂ and 3% O₂. Xenon is used for its high efficiency to absorb TR photons of typical energy 6–15 keV. The space between the straws is filled with radiator material. The TR photons (soft X-rays) emitted in the radiator are absorbed in the gas inside the straw tubes, which serve as detecting elements both for tracking and for particle identification (more

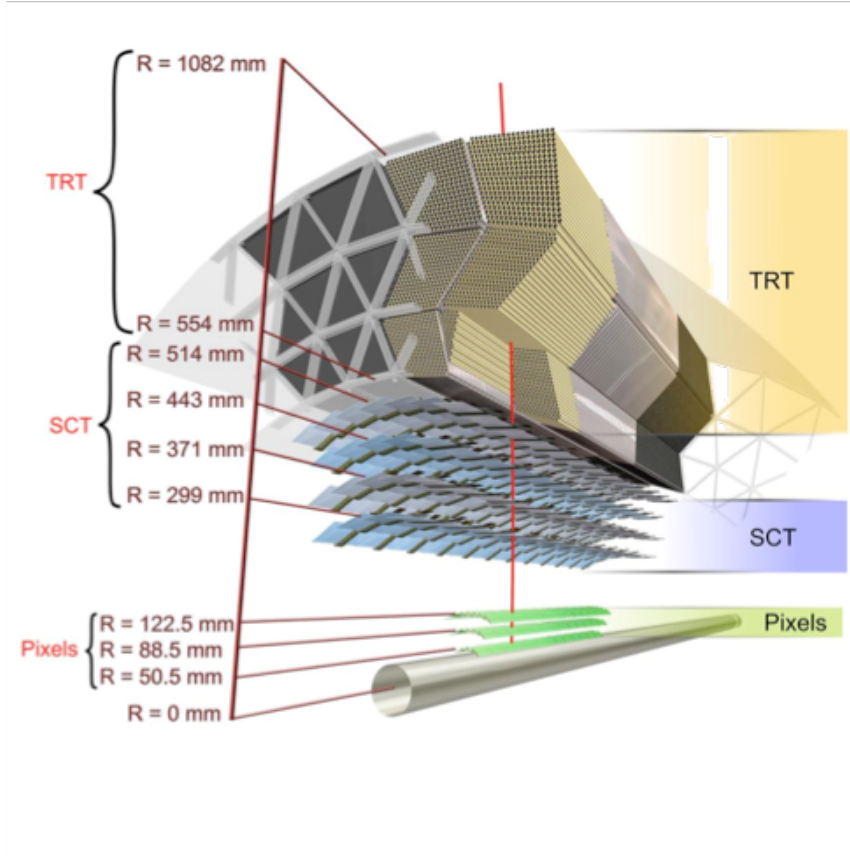


Figure 1. Schematic view of the Barrel part of the ATLAS Inner detector.

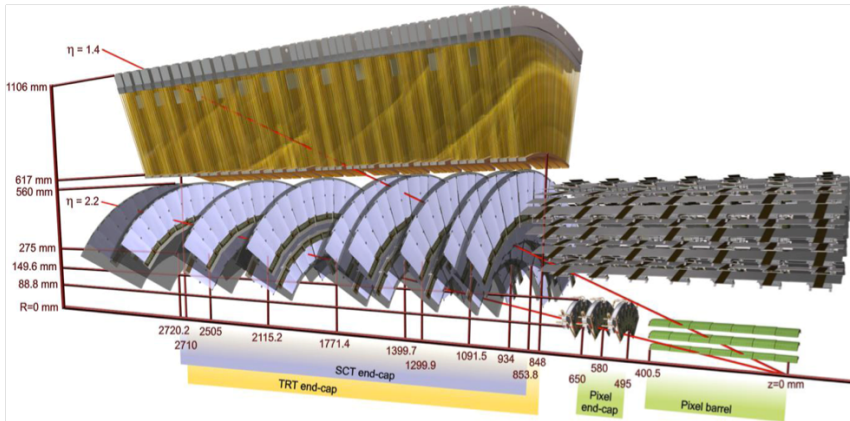


Figure 2. Schematic view of the End Cap (EC) part of the ATLAS Inner detector.

about TRT performance can be found in [5]). The straw wall is held at a potential of about -1530 V with respect to a 31 μm diameter gold-plated tungsten wire at the centre that is referenced to ground. The electrons drift towards the wire and cascade in the strong electric field very close to the wire with a coefficient of 2.5×10^4 (gas gain), thus producing a detectable signal. The signal in each wire is amplified, shaped and discriminated against two adjustable thresholds: the Low Level (LL)

threshold (~ 300 eV), is used to calculate the track to anode wire distance by measuring the drift time of the closest electron cluster to the wire and the High Level (HL) threshold (~ 6 keV) used to identify a large energy deposits from absorbed TR photons for particle identification.

The low level threshold is set to a minimum defined by the rate of electronics noise pulses. Any increase of this threshold leads to a worsening of the drift time accuracy measurement. For instance, an increase of the LL threshold by 20% leads to a change of a coordinate accuracy from $125\text{ }\mu\text{m}$ to $130\text{ }\mu\text{m}$ and to a reduction of drift time measurement efficiency by 5% [6].

Particle separation is based on probability to exceed the high level threshold. This probability is different for particles which produce TR (Lorentz γ factor above ~ 500) and other particles with a γ factor below ~ 500 . This probability is highly sensitive to the value of the threshold. It has been shown that TRT particle separation power stays the same if the variation of the effective threshold across the detector is stable to within 20% [5]. This constraint seems loose but it must be maintained against all possible uncertainties like signal amplitude variations along the straws, electronics channel to channel gain variations, gas gain variations etc. Some of these sources of amplitude variations are quite stable over time and can be partially compensated by regular calibration procedures. However there are other sources of amplitude variation for which the environmental change is too short of a time (hours) to be compensated by an offline compensation procedure. The gas gain is sensitive to three such varying parameters: the gas pressure, gas temperature and gas composition. Since these parameters can and do change over the course of a run, a real-time hardware compensation system to adjust the high voltage on the straws called the Gas Gain Stabilisation System was developed. Apart from global variations of temperature and pressure there are local variations of temperatures within the TRT detector volume which also must be compensated.

During the Large Hadron Collider (LHC) collisions the ionisation currents generated within straws are sufficiently large such that they heat the gas inside the straws and temperature within the detector becomes dependent on the LHC luminosity leading to an unavoidable time dependence of the gas gain of the course of each run. The design of the ATLAS inner detector assumed thermal neutrality of neighbouring subdetectors. That is, the design tried to keep the inevitable heat production (e.g. electronics, ionisation in straws) confined within the originating subsystem until it could be removed by a cooling system. Thermal barriers between the TRT, which run at room-temperature and the silicon detectors, which run well below 0°C , were foreseen by design but do not guarantee a uniform temperature distribution across the TRT detector volume. In order to compensate the effect of the temperature on the gas gain, each partition of the TRT (2 barrel, 2 end-cap) is equipped with 236 temperature sensors. Data from these sensors is used to adjust the TRT high voltages in real time.

This paper describes in detail the concept and implementation of the TRT gas gain stabilisation. The design requirement to control the gas gain time variation in all TRT straws is determined such that the effective threshold variation is below $\sim 5\%$.

2 Gas gain stabilisation in the ATLAS TRT

The ATLAS TRT Gas Gain Stabilisation System maintains gas gain stability throughout the TRT by using the Detector Control System (DCS) [7, 8, 13] to adjust in real time the high voltage (HV) in ~ 2000 TRT HV partitions. The GGSS produces the single reference voltage (HV_{ref}) that compensates for variations in the actual composition of active gas as well as its temperature and

pressure. The TRT has a completely closed loop active gas system which constantly adjusts the gas composition sent to the detector. The GGSS draws sample gas directly from the TRT gas system closed loop return manifold guaranteeing that the HV adjustments are based on the actual flow condition of the active gas. The GGSS operates at atmospheric pressure while the gas pressure in the TRT is regulated to be within a few tens of *mbar* above atmosphere. Since the working gas composition and pressure are essentially the same within the GGSS and throughout the entire TRT, only variations in temperature across the detector need to be taken into account when calculating the high voltage settings for different regions of the detector. The number of temperature sensors used for stabilisation purposes is far less than the number of HV partitions, hence, the detector has to be divided into regions which are chosen according to the sensor topology and mechanical granularity (see figure 3).

The TRT Barrel is divided into 4 ϕ sectors ($\pm 45^\circ$) and into the 3 layers of barrel modules and thus, the barrel contains 12 regions where the HV is regulated independently following temperature measurements. Each of these 12 regions has 3 temperature sensors along Z near the outside radius of the region. The average of these 3 measurements is taken as 'regional temperature' used for HV correction (see also figure 3a).

The TRT end-caps form stacks of wheels that for stabilisation purposes are divided in ϕ into 4 sectors ($\pm 45^\circ$) and into the number of wheels in Z (14) and thus each end-cap contains 56 regions (see figure 3b). Each of these regions have sensors on their front and back in Z and the average of these two sensors is taken as representative for the region.

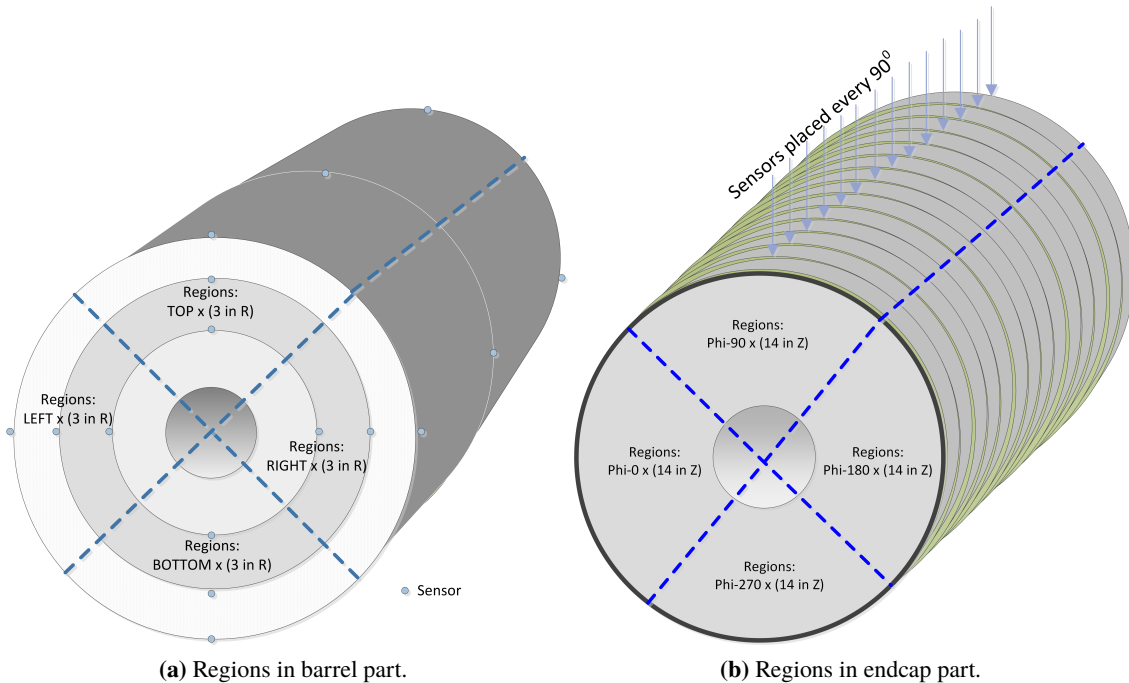


Figure 3. Detector segmentation used for the TRT gas gain stabilisation based on the detector temperature information.

The temperature inside the GGSS system is quite stable and measured with an accuracy of about 0.1 °C, while the temperature variations within the TRT detector are much larger. Within an hour of powering the electronics, the temperatures across the detector start to stabilise. However, at different regions of the TRT the temperature variation is significant (6-9°C). During the course of a run, regional temperatures are varying depending on local particles fluence and amount of ionisation deposition hence the variations must be compensated for in real time. The single reference voltage value produced by GGSS system is sent to the TRT DCS HV controllers where the HV for each detector region is recalculated and set according to the following formula:

$$HV_{\text{cor}} = HV_{\text{ref}} + \alpha(T_{\text{reg}} - T_{\text{ggss}}) \quad (2.1)$$

where: HV_{cor} is the voltage to be applied in region, HV_{ref} reference voltage, α is thermal coefficient of the active gas and T_{reg} and T_{ggss} are the regional and the GGSS temperatures respectively. To protect the TRT sensors (i.e. straws) against failures of the GGSS and dangerous environmental conditions, the TRT HV DCS system has several protection mechanisms. The calculated setting is compared to a *maximum* voltage value protecting the detector against overvoltage. If an overvoltage setting is requested, the HV is set to the maximal value. The GGSS also sends HV_{ref} quality flags after every measurement cycle to provide information whether voltage value is to be trusted or not. If any of these flags are true, the TRT HV is not changed.

3 Operation principles of the Gas Gain Stabilisation System

GGSS operation is based on a stabilisation of the signal amplitude produced by ^{55}Fe X-rays in reference (test) straws. The operation of proportional gaseous counter is thoroughly explained in basic textbooks and the key parameter governing this is the value of the gas gain A , ($A = n/n_0$) (where n_0 is number of primary ion pairs liberated in active gas). Changes in the peak position of the pulse height spectrum of the 5.9 keV X-ray emission line of a ^{55}Fe source irradiating reference straws are interpreted as changes in the gas gain. The high voltage on the reference straws is adjusted to maintain the fitted peak at a fixed average value that defines the design gas gain value. After each measuring cycle, the reference voltage is recalculated to maintain the design gas gain and then sent to the DCS which then adjusts the high voltage in each TRT region taking into account the local temperature. The steps by which the high voltage is modified to maintain the nominal gas gain are as follows (see also figure 4):

- the starting values for the high voltage (HV_s) and peak position (pp_s) are manually entered to initialise the GGSS when it is turned on (the default values are selected to be typical values for the TRT straws),
- the spectrum of ^{55}Fe is collected for the currently set HV ,
- peak position — pp_c , energy resolution, and skewness are calculated using a Gaussian fit of the spectrum,
- bad measurements are rejected using the calculated energy resolution and skewness,

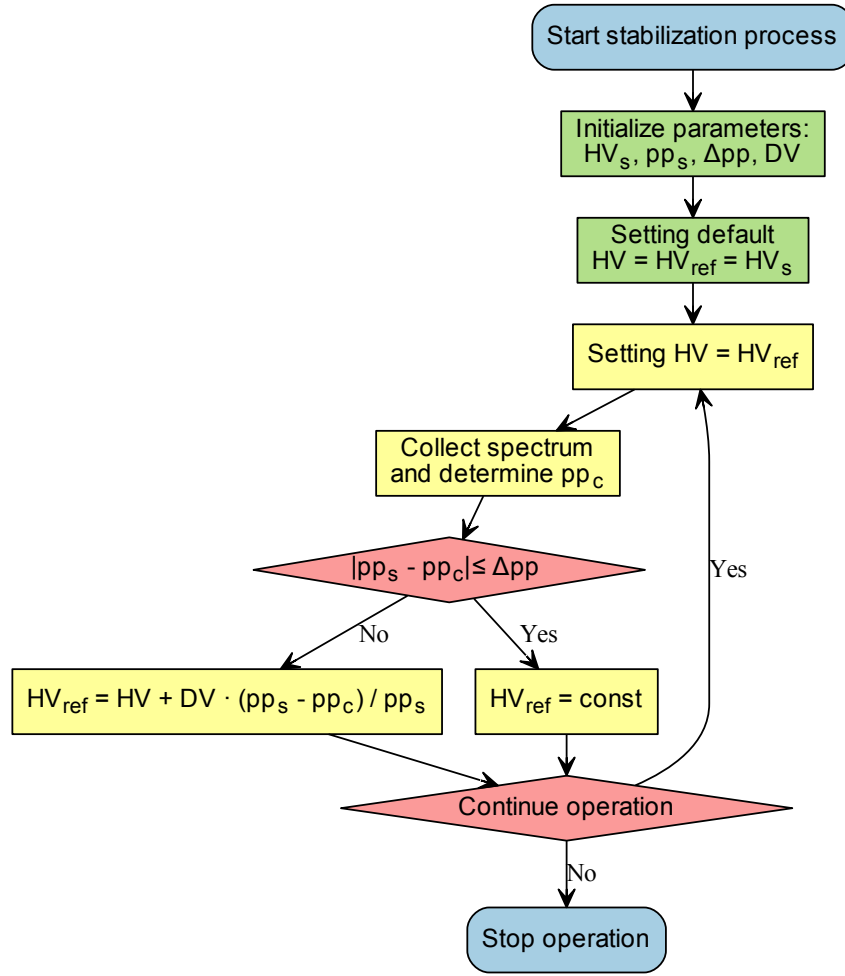


Figure 4. Simplified block diagram of the GGSS operation.

- once a good measurement is obtained, the new HV value is calculated from the formula:

$$HV = HV_s + \frac{pp_s - pp_c}{pp_s} DV \quad (3.1)$$

where DV is the voltage needed to double the gas gain (i.e. 70 V),

- the new value of the HV is applied to the test straw and the procedure is repeated until the condition $|pp_s - pp_c| \leq \Delta pp$ is met (where: Δpp is the required accuracy of peak position stabilisation, in this case is equal to 10% of pp_s),
- when $|pp_s - pp_c| \leq \Delta pp$ is achieved, the procedure then sets $HV_{ref} = \overline{HV}$, where HV_{ref} is the voltage sent to DCS. To ensure robustness of the HV_{ref} value it is calculated as the mean, \overline{HV} , of the values obtained in each of the reference straws (using only straws with good values).

4 Properties of the reference straw tubes and related components

Stable operation of the GGSS is a key factor for successful TRT operation. Significant work has been carried out to ensure good knowledge of the performance of the basic components of the system and study their properties. The straw tubes used as reference detectors have been carefully examined and were selected for the uniformity of their response. The following parameters were measured in selecting the final straw tubes used in the GGSS:

- the gas gain as a function of high voltage and position of radiation source along the straws,
- the counting characteristics (i.e plateau curves),
- the gas gain response to pressure and temperature variations,
- the energy resolution, measured as ^{55}Fe spectrum peak width,
- the long-term stability,
- minimal change in straw tube operation from radiation-induced ageing.

4.1 Gas gain measurements

The gas amplification (gain) is a function of the high voltage applied to the straws and gas amplification factors ranging from 1 to 7×10^5 , were determined using a current measurement technique for various gas mixtures (see table 1). The gas gain A was determined from the ratio I/I_0 , where I and I_0 are the measured currents for a constant flux of X-ray photons for the applied voltage and for the ionisation chamber regimes (the HV value when all ionisation is collected on the anode without gas gain), respectively. All measurements have been performed at atmospheric pressure. In order to eliminate space charge effects, the measured current was kept below 1 nA. The accuracy of gas gain measurements is limited by the currents measurements and do not exceed 5%. The results shown in figures 5a and 5b are for the full set of studied gas mixtures.

Table 1 shows the maximum safe operating gas gain for all studied gas mixtures. Above this value, the probability of self quenched (limited) streamers (SQS) becomes significant which leads to an increase of discharge probability.

Table 1. Maximum gas gain for a safe straw operation.

Gas mixture	Highest safe gas gain
Ar/CO ₂ 80/20	4.9×10^4
Ar/CF ₄ /CO ₂ 70/20/10	2.4×10^4
Ar/CO ₂ /N ₂ 80/10/10	3.7×10^4
Xe/CO ₂ 70/30	7.4×10^4
Xe/CF ₄ /CO ₂ 70/20/10	7.2×10^4
Xe/CO ₂ /O ₂ 70/27/3	9.8×10^4

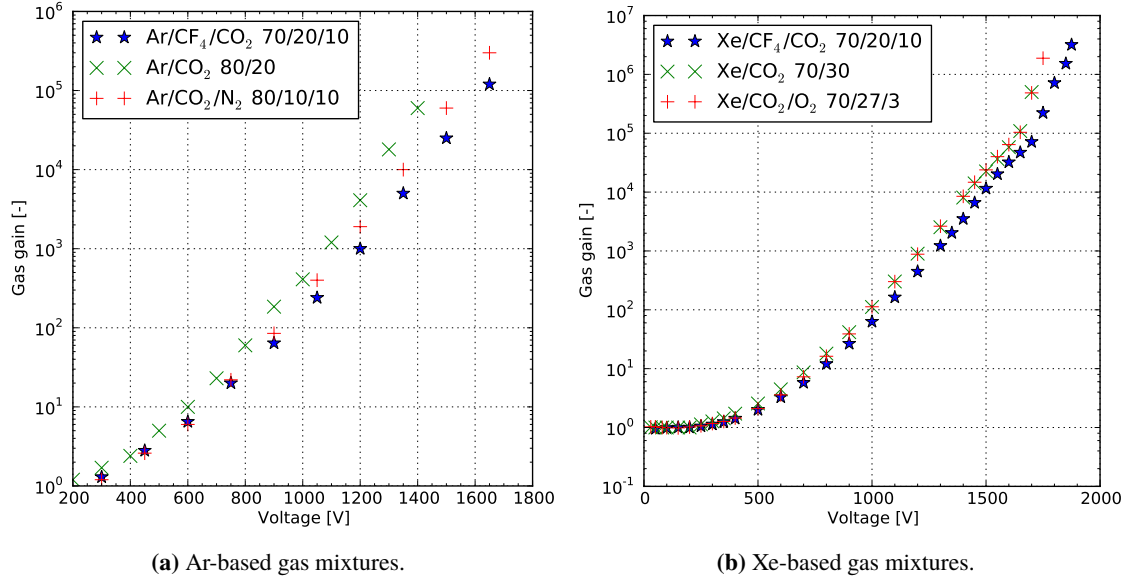


Figure 5. Gas gain as the function of voltage applied between anode and cathode of straws for studied mixtures, $p=1030$ hPa, $T=293^\circ\text{K}$.

The energy resolution (FWHM) has also been measured as a function of the applied voltage. The results obtained are presented in figure 6a, 6b and table 1. Energy resolution worsens close to the gas gain safety limit. In order to ensure maximum stability of the GGSS, the working point was chosen to be slightly below the nominal TRT gas gain of 2.5×10^4 .

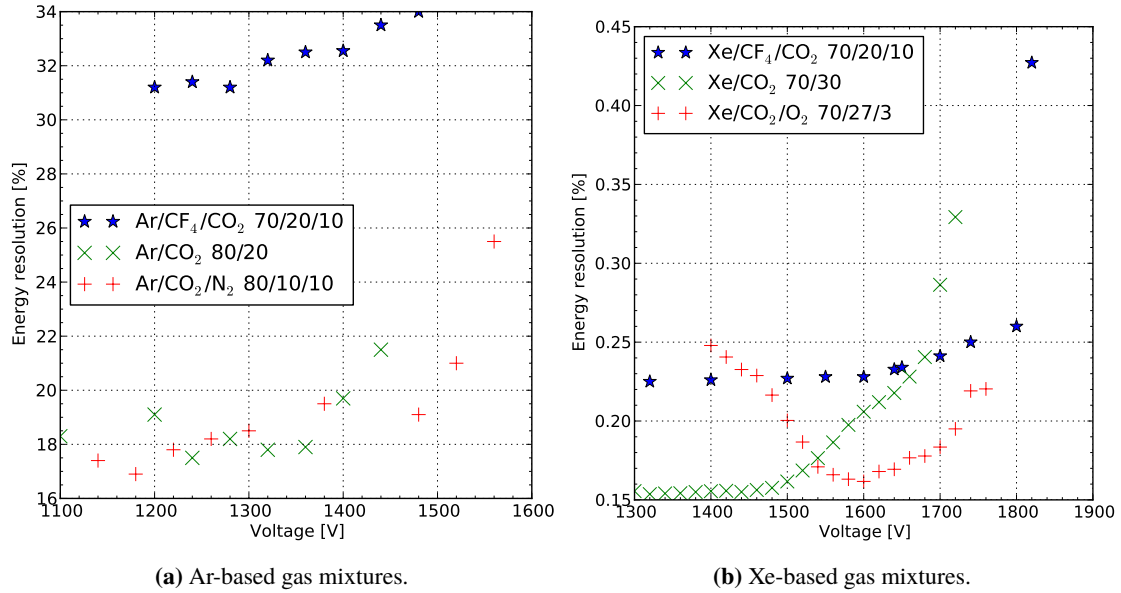


Figure 6. Energy resolution for 5.9 keV ^{55}Fe X-Ray line as a function of anode voltage for different gas mixtures.

4.2 Gas gain temperature dependence

The electron amplification process near the wire is very sensitive to the density of the working gas and thus to both temperature and pressure variations. A temperature change of $\Delta T = 1^\circ\text{K}$ at 293°K causes a change of gas pressure $\Delta p = 3.53\text{ hPa}$ at a pressure of $p = 1035\text{ hPa}$. While both the TRT and the GGSS operate at atmospheric pressure, gain variations caused by temperature differences can be significant and are compensated by applying HV corrections for each TRT region separately. The influence of temperature on the gas gain was studied in straw tubes from 15°C to 45°C for the 80/20 Ar/ CO_2 gas mixture and the TRT baseline gas mixture (Xe/ CO_2/O_2 70/27/3). A special set-up which provided a thermal stability of 0.1°C was used for the temperature dependence study. The results of this study are presented in figures 7a and 7b which show the high voltage adjustment needed to compensate the temperature differences. As seen in figure 7, the temperature dependence of peak position (and thus the gas gain) can be accurately approximated by straight line. The thermal coefficient of the gas gain (pulse height) is $-1.54\text{ V}/^\circ\text{C}$ for the 80/20 Ar-based gas mixture and $-2.13\text{ V}/^\circ\text{C}$ for the TRT baseline mixture Xe/ CO_2/O_2 (70/27/3).

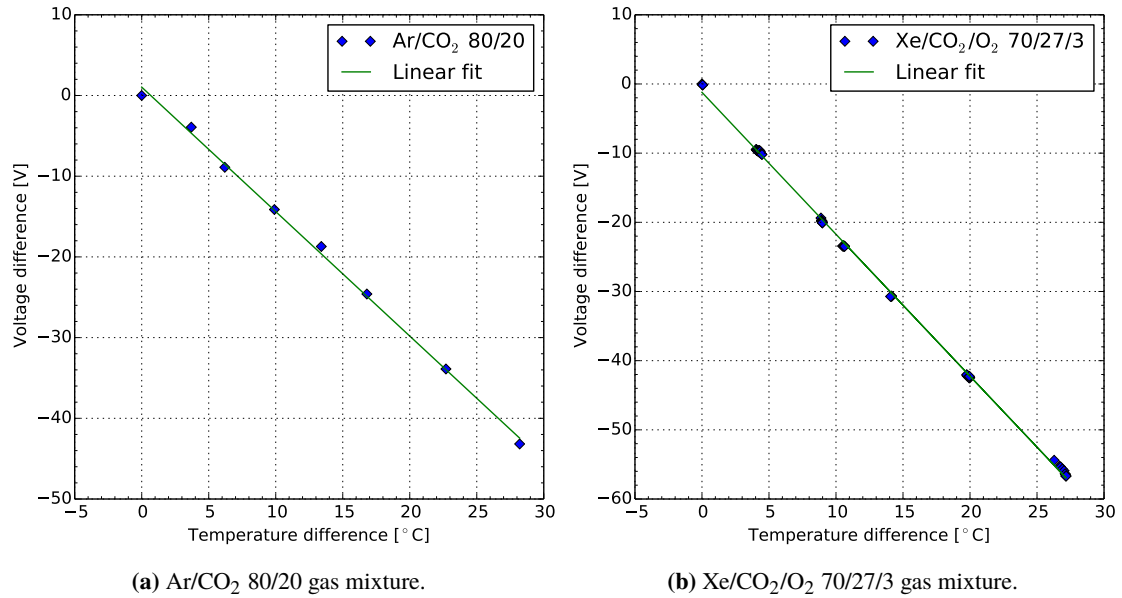


Figure 7. Voltage adjustment needed to keep a constant gas gain as a function of a temperature change (the lower temperature was 15°C).

5 Design of the Gas Gain Stabilisation System

5.1 Hardware

The TRT GGSS consists of:

- two reference detectors with eight straws (15 cm in length) each enclosed in a brass box,
- 16 preamplifiers — one for each straw,

- three high voltage power supplies and three DAC's for their control (12 channels in total),
- two analogue signal multiplexers,
- two spectroscopic amplifiers,
- two multichannel analysers (MCA),
- and a control PC.

The straws are mounted inside a gas tight brass box that is equipped with gas inlet and outlet manifolds which supply the straws with active gas in parallel. The straws (the cathodes) are connected to the ground and the central wires (the anodes) connected to individual high voltage lines and preamplifiers. The straws run at a slightly lower voltage (50 V) than the detector to minimise radiation induced ageing. There are two PT1000 sensors measuring active gas temperature with accuracy of $\sim 0.1^\circ$. Each box has a gas tight Kapton window in its cover separating the straws and ^{55}Fe source. The signals generated by the straws are preamplified, then multiplexed to the spectroscopic amplifier, before finally being sent to a Multi Channel Analyser (MCA) for analysis. Because of the critical role of the GGSS in the TRT operation, every component has at least one hot spare. During normal operation only one box is used and a second fully-equipped box provides a redundant backup in case of problems. A simplified schematic view of all major GGSS modules and their interconnections are shown in figure 8. To monitor all critical working parameters (temperatures, gas flow, etc.) an Embedded Local Monitor Board (ELMB) is used [11]. It has 64 input analogue channels from which information is send to the DCS for long term storage to allow historical trend monitoring.

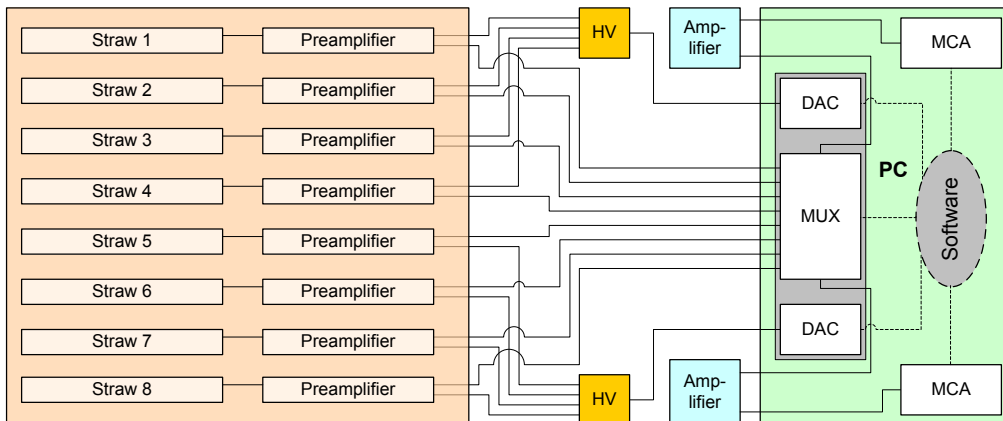


Figure 8. Block diagram of the GGSS; Straw (1-8) — four stabilisation, two monitored and two spares; Preamplifier — charge sensitive, home made; HV — high voltage power suppliers CAEN model N472; Amplifier — ORTEC model 575A; DAC - digital analogue converters — MEN Mikro Elektronik GmbH model M37; MUX — analogue multiplexer — MEN Mikro Elektronik GmbH model M56; MCA — multichannel analyser — ORTEC model MCB — Trump PCI 2k.

5.2 Software

Dedicated control software for the GGSS is integrated into the TRT DCS [13] and hence the global ATLAS control system. The core GGSS control application is written in C++ and runs as a service on a dedicated computer. The application communicates exchanging data and commands with DCS via the Distributed Information Manager (DIM) [12]. The software is responsible for the configuration and control of hardware components, data collection of measurements, and validation of calculated results. The outputs sent to DCS are the reference high voltage, the gas temperature, and their quality flags as well as any warnings or errors reported by the system.

A sketch of a simplified schema of software modules is shown in figure 9. The GGSS software uses signals from four “stabilisation” straws to compute a new value of the reference high voltage. The system collects spectra sequentially (using the multiplexer which routes the signals to the amplitude analyser). When the spectra of all four “stabilisation” straws are measured, a new value of reference high voltage is computed as the mean value of the high voltages calculated for the correctly working stabilisation straws. The reference voltage is then applied to additional “monitored” straws to check that its value results in the correct signal peak position. This cross-check is also used for longterm monitoring of the system behaviour. The whole procedure (which takes ~ 10 min) is repeated continuously as long as the GGSS is in operation. There are also two spare straws in the GGSS box which are to be used in case of problems with any of the “stabilisation” straws.

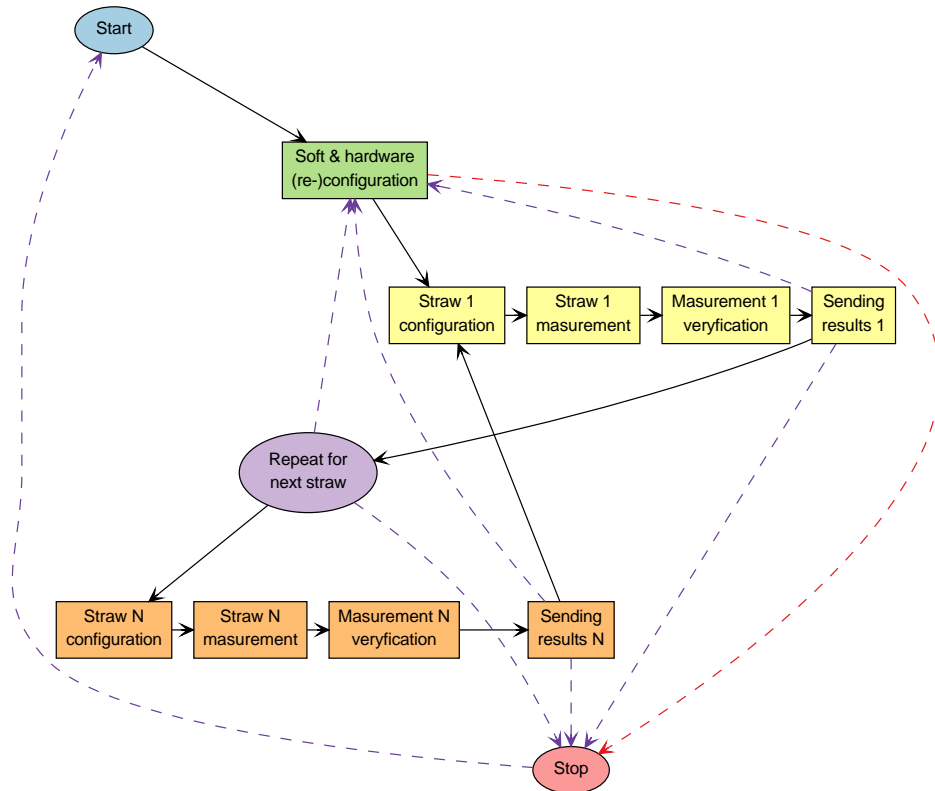


Figure 9. Simplified block diagram of software.

6 Longterm system performance

For the entire LHC Run-1 (almost four years) the GGSS operated continuously during all periods of ATLAS physics data taking.

6.1 Reference high voltage

The reference voltage is calculated using GGSS operation voltage and the known dependence of the gas gain on voltage. Under stable operating conditions HV_{ref} depends only on temperature and atmospheric pressure but will also react to gas mixture composition variation and changes to other parameters. A *normalised high voltage* (HV_{norm}) value was introduced in order to monitor the operation parameter stability. It is calculated using *first principles* using following formula:

$$HV_{\text{norm}} = (HV_{\text{start}} + \Omega_T(T - T_{\text{start}}) + \Omega_p(p - p_{\text{start}})) \quad (6.1)$$

where HV_{norm} is the normalised high voltage as function of the temperature T and pressure p . The parameters in the formula are HV_{start} the reference high voltage (1483.8 V), T_{start} the reference gas temperature (23.6°C), p_{start} the reference pressure (976.5 hPa), Ω_T the temperature coefficient (−2.13 V/°C), and Ω_p the pressure coefficient (0.55 V/hPa). The parameters shown were measured when the detector was running in optimal conditions at 2009-10-25 23:00:00. Figure 10 shows the longterm behaviour of the reference (green line) and normalised (red line) high voltages as well as their difference (blue line) where this difference should ideally be *zero*. Significant deviation from *zero* usually indicates a problem with the gas composition. For instance after restarting the detector in 2010 this difference reached a level of almost 40 V caused by a miscalibration of the gas analyser which was used for active gas mixture control. This event demonstrates another important function of the GGSS — monitoring the stability of the detector gas mixture which is critical to the proper TRT operation.

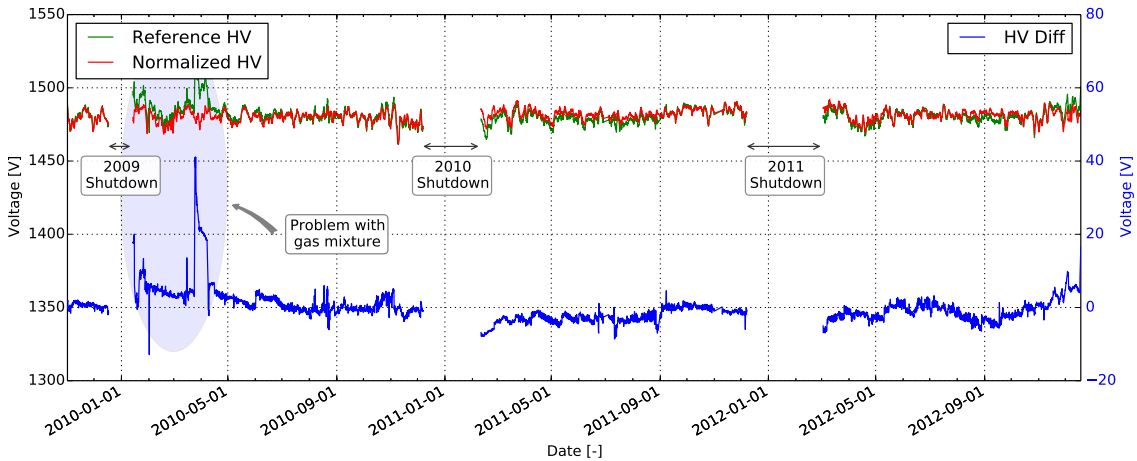


Figure 10. Reference and normalised HV (left black scale/red and green lines) and their difference (right blue scale/line) during GGSS performance over the three and a half year period from December 2009 to March 2013.

6.2 Gas gain stability

The historic trend of the peak position for one of the stabilisation straws and for one of the monitoring straws over a period of about 2 years is shown on figures 11 and 12. One sees an excellent stability with the ^{55}Fe line position maintained within $\pm 1\%$ for one of the gas gain stabilisation straws. The peak position for monitoring straw, figure 12, over long period of time is also stable within $\pm 1\%$ except for some deviations that were caused by miscalibration of a high voltage power supply. Atmospheric pressure is a major factor of the the gas gain variation and figure 13 shows a variation of HV_{ref} (black curve) compared to the variation of atmospheric pressure (blue curve).

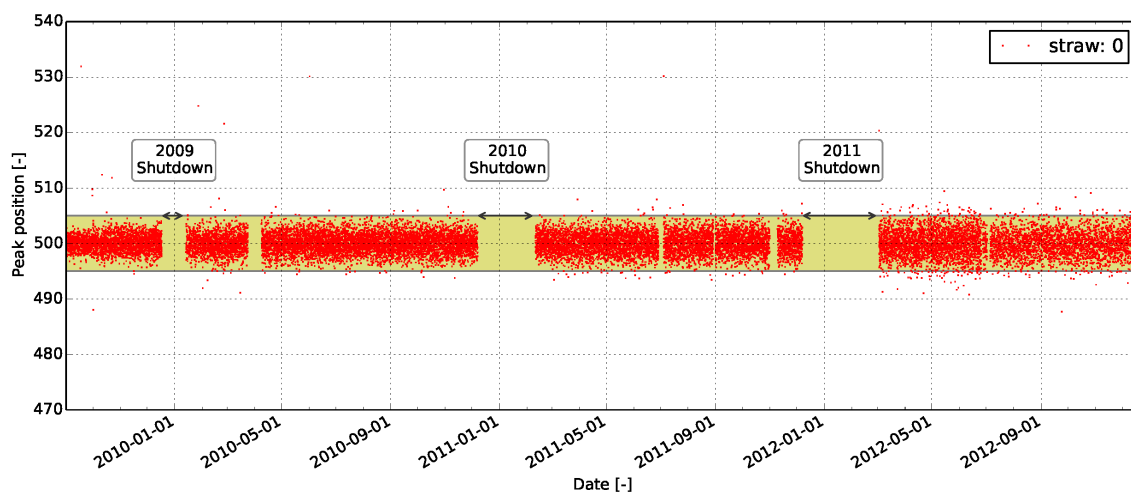


Figure 11. Peak position of ^{55}Fe line for straw used for gas gain stabilisation (a highlighted region represents $\pm 1\%$ range).

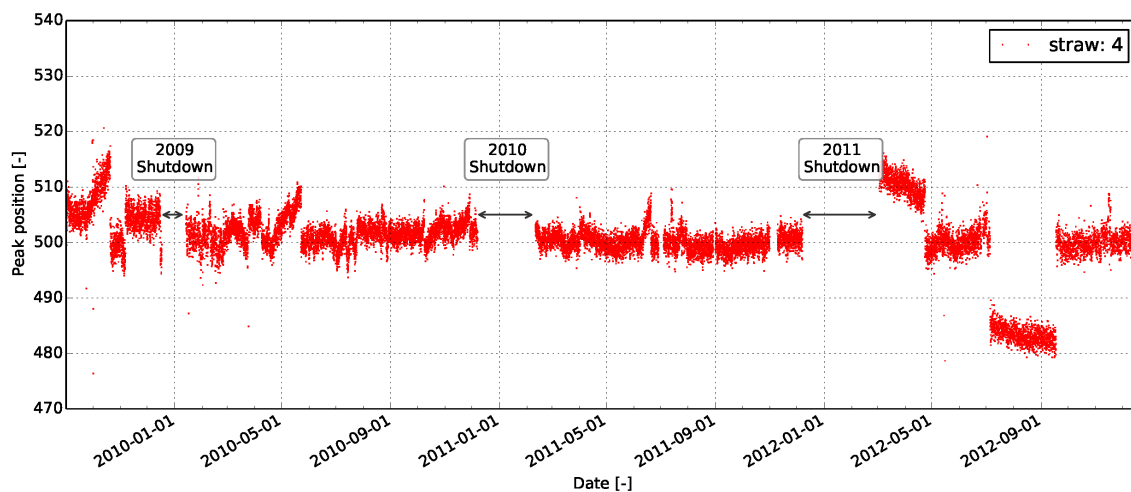


Figure 12. Peak position of ^{55}Fe line for monitoring straw.

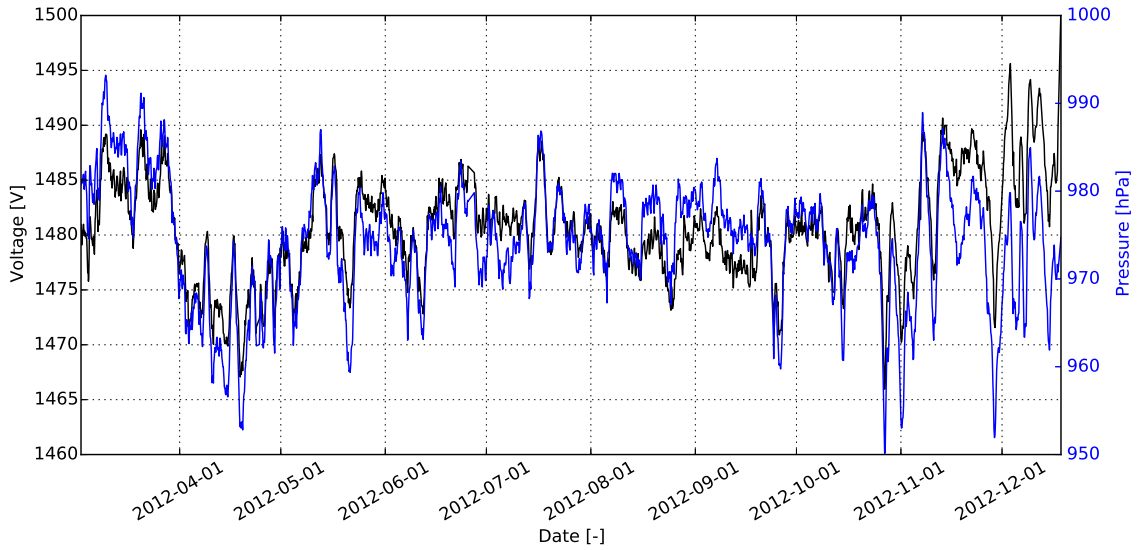


Figure 13. Longterm trends of crucial GGSS parameters: HV_{ref} (black) and gas pressure (blue) in 2012; one can observe the expected strong correlation between the two.

In 2012, the luminosity of LHC reached a value where deposited ionisation in straws started to cause noticeable heating. Figure 14, shows TRT HV setting for one of the barrel HV region for a 20 hour period during which there were two LHC fills producing significant numbers of collisions. From the top to bottom plot (a) shows the current in one barrel HV line which follows LHC instantaneous luminosity, plot (b) shows temperatures measured by probes in one barrel region, plot (c) shows variation of the applied high voltages in the same barrel region and plot (d) shows the value of HV_{ref} received by DCS from the GGSS.

Electron separation from a hadron background is calculated from the fraction of straws crossed by a track with energy deposition above ~ 6 keV, the high level hit fraction. For electrons this fraction is about $\sim 25\%$ and for pions it is $\sim 5\%$. In order to suppress pions, a cut on this parameter of about $\sim 15\%$ is applied so that a track with a high level hit fraction of more than 15% is considered to be an electron track. This cut allows rejections of $\sim 95\%$ of pions at a price of an $\sim 10\%$ loss of electrons. The cut is a part of software analysis tool and is not expected to change during data taking. Any significant change of the gas gain would lead to a change of high level hit fraction on particle track and hence to change in the fraction of pions which pass the cut along with change in electron acceptance efficiency. A change of the gas gain by 10% leads to a change of high level hit fraction by 20% . Figure 15 shows a variation of the HL fraction during the 2011 running period. One sees that HL hit fraction varies by $\sim 3\%$, which corresponds to the gas gain variation of $\sim 1.5\%$ within the TRT detector.

7 Conclusions

The excellent stability of the TRT during Run-1 to a large extent resulted from the TRT GGSS system maintaining nearly constant gas gain over the entire running period. Beyond maintaining stable gas gain in all parts of the TRT, the GGSS provides an efficient monitoring tool to detect

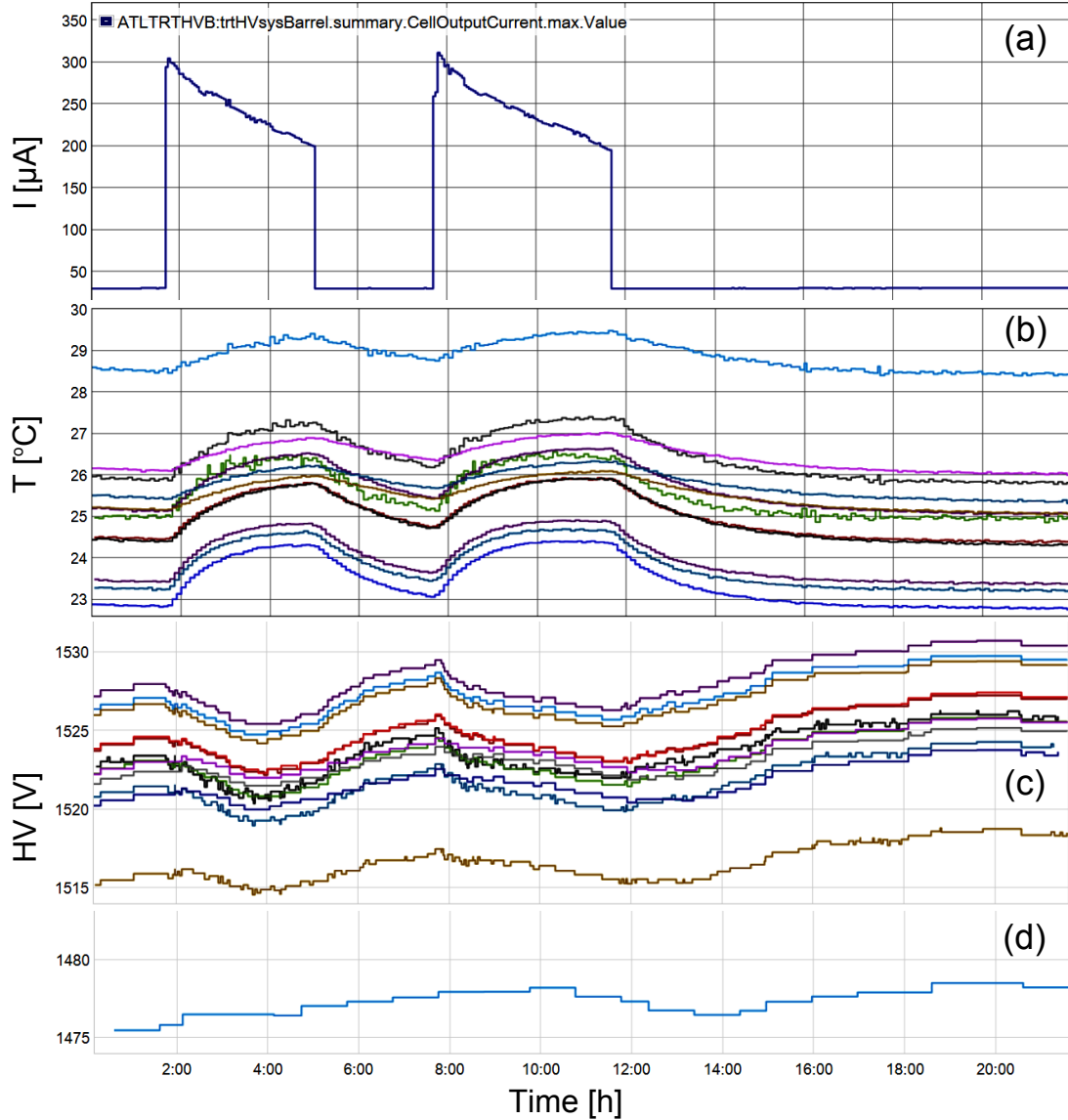


Figure 14. Current in one HV channel of the TRT (a); Trends of the temperature in one of the barrel TRT regions (b); High voltages applied to the same barrel region HV_{cor} (c); the GGSS voltage HV_{ref} (following the atmospheric pressure) (d).

changes in the gas mixture composition not detected by other analysis devices of the TRT gas system. It should be emphasised that during Run-1, GGSS was operating 100 % of the time when the TRT and ATLAS were taking physics data. To the date of this publication, the GGSS has not had a single fatal failure proving the robustness of the system design and of the methods and components chosen to build the system.

The GGSS has proven to be a key and very reliable component of the TRT detector meeting all design goals: system reliability confirmed by no fatal failures, accuracy of the gain stabilisation well within the range of $\sim 1\%$. Moreover the GGSS is very sensitive to any active gas mixture changes, therefore it acts as a fast and accurate “sensor” of problems related to the active gas.

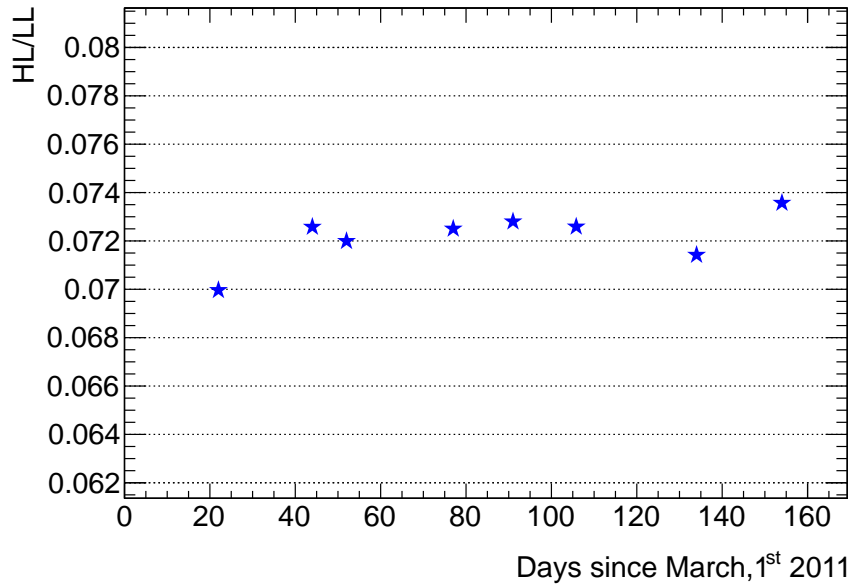


Figure 15. Variation of HL hit fraction on particle track during the 2011 running period.

The GGSS has contributed significantly to the global quality of the data acquired by the TRT detector and hence by whole ATLAS experiment. This was achieved by keeping the gas gain in the TRT detector within $\sim 1.5\%$ stable range, therefore HL hit fraction variation was reduced to about $\sim 3\%$, which significantly contributes to the high capability of the particle identification in the ATLAS experiment.

After a successful major GGSS upgrade during the Long Shutdown 1 of the LHC, the system was ready for Run-2 physics data taking period and continues its operation.

Acknowledgments

This work was supported in part by the Polish National Science Centre, grant no. DEC-2013/08/M/ST2/00320. This work was supported in part by the Turkish Atomic Energy Authority.

References

- [1] ATLAS collaboration, *The ATLAS Experiment at the CERN Large Hadron Collider*, [2008 JINST 3 S08003](#).
- [2] ATLAS TRT collaboration, *The ATLAS Transition Radiation Tracker (TRT) proportional drift tube: design and performance*, [2008 JINST 3 P02013](#).
- [3] ATLAS TRT collaboration, *The ATLAS TRT end-cap detectors*, [2008 JINST 3 P10003](#).
- [4] ATLAS TRT collaboration, *The ATLAS TRT Barrel Detector*, [2008 JINST 3 P02014](#).
- [5] E. Hines for ATLAS collaboration, *Performance of Particle Identification with the ATLAS Transition Radiation Tracker*, in *Proceedings of Meeting of the APS Division of Particles and Fields (DPF 2011)*, Providence U.S.A. (2011) [[arXiv:1109.5925](#)].

- [6] T. Akesson et al., *Straw tube drift-time properties and electronics parameters for the ATLAS TRT detector*, *Nucl. Instrum. Meth. A* **449** (2000) 446.
- [7] K. Lantzsch et al., *The ATLAS Detector Control System*, *J. Phys. Conf. Ser.* **396** (2012) 1.
- [8] A. Barriuso Poy et al., *The detector control system of the ATLAS experiment*, *2008 JINST* **3** P05006.
- [9] ATLAS TRT collaboration, *The ATLAS TRT electronics*, *2008 JINST* **3** P06007.
- [10] T. Akesson et al., *Particle identification using the time-over-threshold method in the ATLAS Transition Radiation Tracker*, *Nucl. Instrum. Meth. A* **474** (2001) 172.
- [11] B. Hallgren et al., *The embedded local monitor board (ELMB) in the LHC front-end I/O control system*, at *Electronics for LHC experiments*, Stockholm Sweden (2001), pg. 325.
- [12] C. Gaspar and B. Franek, *Tools for the automation of large distributed control systems*, *IEEE Trans. Nucl. Sci.* **53** (2006) 974.
- [13] J. Olszowska et al., *The ATLAS Transition Radiation Tracker (TRT) Detector Control System*, in *Proceedings of ICALEPCS 2011*, Grenoble France (2011), pg. 666.